Research Article

Abdullah M. Zeyad*, Khaled H. Bayagoob, Mohamed Amin, Sahar A. Mostafa, and Ibrahim Saad Agwa

Influence of nanomaterials on properties and durability of ultra-high-performance geopolymer concrete

https://doi.org/10.1515/rams-2024-0071 received May 15, 2024; accepted November 06, 2024

Abstract: This study examines the effect of adding different dosages of nontitanium (NT) and nano-silica (NS) ranging from 0.5 to 4% by weight of binder materials on ultrahigh-performance geopolymer concrete (UHPGC). The material's feasibility was evaluated using slump flow measurements. A detailed analysis of its compressive strength (CS), transport properties, and sulfate attack was conducted. The addition of 2.5% NS and 4% NT improved the CS and transport properties of UHPGC compositions, creating a denser and more durable microstructure with enhanced interfacial bonding, as confirmed by the microstructure study. According to this study, the most effective doses for enhancing UHPGC performance in various aspects are 2.5% NS and 4% NT. The CS was recorded at 198.7 MPa for 2.5% NS mixes and 197.6 MPa for 4% NT mixes for ages test 28 days. These findings provide valuable insights into developing and utilizing advanced, high-efficiency UHPGC for sustainable and sturdy construction techniques.

Keywords: UHPGC, nano-silica, nano-titanium, compressive strength, transport properties, sulfate attack, ultrahigh-performance geopolymer concrete

Khaled H. Bayagoob: Department of Civil Engineering, College of Engineering, University of Bisha, P.O Box 61922, Bisha, Saudi Arabia **Mohamed Amin:** Department of Civil and Architectural Constructions, Faculty of Technology and Education, Suez University, Suez, 43221, Egypt; Civil Engineering Department, Mansoura Higher Institute of Engineering and Technology, Mansoura, Egypt

Sahar A. Mostafa: Department of Civil Engineering, Faculty of Engineering, Beni-Suef University, Beni-Suef, Egypt

Ibrahim Saad Agwa: Department of Civil and Architectural

Constructions, Faculty of Technology and Education, Suez University, Suez, 43221, Egypt

1 Introduction

The cement-based concrete industry is struggling to keep up with the growing demand for cement. It faces many challenges, such as environmental damage due to carbon dioxide emissions, limited limestone reserves, high energy consumption, and slow manufacturing growth. Efforts are being made to find alternative binders to traditional Portland cement to reduce its production and the use of non-renewable natural resources. Researchers are exploring the use of pozzolanic waste and materials as partial cement replacements to enhance concrete performance. Another area of recent study is the development of concrete using alkaline-activated bond systems (geopolymer bonds). Alkaline activation of aluminosilicate powder results in the formation of inorganic geopolymer bonds.

Geopolymer bonds combine the polymer and cement properties [1]. Silica and alumina react in an alkaline medium to create a three-dimensional polymer chain through polycondensation, forming Si–O–Al–O bonds [2]. Metakaolin, fly ash (FA), and blast furnace slag are commonly used to make geopolymer concrete [3]. Geopolymer concrete (GC) efficiency depends on activators, aluminosilicate types, mixing ratios, and curing methods [4]. GC is a promising substitute for cement-based concrete. It has low permeability and high early compressive strength (CS) and can withstand harsh conditions [5]. The production of ultra-high-performance geopolymer concrete (UHPGC) has been accelerated, allowing for the successful use of alkaline-activated technology in structural applications with improved sustainability and durability [6].

The production of UHPGC depends on several key factors, including: (1) engaging silica fume (SF) and Ground granulated blast furnace slag (GGBS) to improve flow properties with low water/binder rates and high activation potentials for alkali [7]; (2) increasing the surface area of the binder particles or adding nanomaterials (NMs) [8]; (3) the use of steel fibers (St.F) and silica sand [9]; and (4) the adoption of the heat treatment method [10]. Ambily *et al.* [8] reported that

^{*} Corresponding author: Abdullah M. Zeyad, Civil and Architectural Engineering Department, College of Engineering and Computer Sciences, Jazan University, Jazan, 45142, Saudi Arabia, e-mail: azmohsen@jazanu.edu.sa

2 — Abdullah M. Zeyad et al. DE GRUYTER

adding SF with GGBS activated with an alkali silicate solution and hydroxide fibers to produced UHPGC containing 2% by volume St.F achieved CS and flexural strength (FS) of 175 and 13.5 MPa in 28 days. This finding is supported by Aydın and Baradan [11], which found that adding SF to GGBS to make UHPGC increased CS by more than 150 MPa when compared to mixtures without SF. According to Wetzel and Middendorf [7], UHPGC with a volume substitution rate of 10-15% of GGBS with SF obtained the highest CS (178.6 MPa). SF dosages of 20-30% were found to reduce GC flowability, despite SF's significant impact on rheological and mechanical properties at higher substitution rates. In another study, Liu et al. [12] reported that increasing the SF6 content from 10 to 30% leads to higher mechanical performance and improves the bond strength between the fiber and the matrix. Moreover, the introduction of UHPGC St.F improves ductility, fracture resistance, and impact resistance. According to Wu et al. [13], the ideal addition of St.F varies from 1 to 3% by volume, which improves the mechanical characteristics of UHPGC in terms of CS and FS. According to Yoo et al. [14], increasing the content of St.F by 2% by volume limits the efficacy of enhancing the characteristics of UHPGC. In fact, it is preferable to keep the fiber content under tight control to minimize workability deterioration and relatively high costs [34].

NM has a significant effect on enhancing the microstructure, decreasing porosity, and boosting the mechanical strength of GC [15]. By incorporating NM into the geopolymer matrix, the properties of concrete are improved, as the nanoparticles can diffuse into ultra-fine pores and function as a filler. In addition, their role in pozzolanic processes leads to increased gel production [16]. Nanoparticles strengthen the bond between binders and assemblies, increase strength properties, prevent cracks, and improve fiber crosslinking [17]. Researchers are focusing their efforts on the incorporation of various NM into the production of UHPGC [18,19]. Nano-silica (NS) [20,21], nano-Al₂O₃ [22], nontitanium (NT) [23–25], nanoclay [26], and carbon nanotubes [27] are among the most frequent of these NM [28]. Incorporating NS into GC typically results in enhanced mechanical performance and increased durability [20]. NS improves concrete properties through active pozzolanic properties and a finer texture that helps fill ultrafine pores, resulting in higher packing density [29,30]. NS was used to decrease concrete permeability while enhancing mechanical properties and resistance to deterioration [19,20]. There is limited information in the literature about how adding NS affects the mechanical performance of UHPGC. Furthermore, it is rare to find information about how NS can enhance the mechanical performance of UHPGC.

The effect of NS on modifying the properties of geopolymers is contingent upon its dosage amounts, particle size,

shape, and degree of dispersion in the geopolymer matrix, as indicated by the previous studies. Consequently, it is possible to conclude that the most effective quantity of NS for modifying the properties of geopolymer composites, such as strength, transport properties, and microstructure, is in the range of 1–3% by mass of alkali-activated materials [31,32].

His study investigates the impact of incorporating different percentages of NT and NS, ranging from 0.5 to 4% of the total weight of binders, on the characteristics of UHPGC. Seventeen mixes were created to investigate the characteristics of fresh, hardened, transport, sulfate attack (SA), and microstructure.

1.1 Research significance

The significance of this research lies in its potential to advance the understanding and application of UHPGC, a material known for its exceptional mechanical properties and durability. By exploring the effects of incorporating NS and NT, this study seeks to enhance the CS of UHPGC, which is crucial for its structural applications. Additionally, this research aims to fill the gap in the existing literature regarding the influence of NS and NT on the transport properties and SA resistance of UHPGC. The findings from this study could lead to significant improvements in the performance and longevity of UHPGC in various environmental conditions, promoting its use in sustainable and resilient construction practices. By providing new insights into the NM modifications of UHPGC, this research could also pave the way for future studies and innovations in the field of advanced concrete technology.

2 Experimental program

2.1 Materials

2.1.1 Ground granulated blast furnace slag (GBFS)

GBFS is a byproduct of the iron manufacturing process. It is formed when the iron foundry cools the slag using water. GBFS was employed to manufacture UHPGC [33,34]. The GBFS was formulated with a consistent density of 730 kg·m⁻³ for all mixtures examined in this investigation. Table 1 displays the chemical and physical characteristics of GBFS.

Table 1: Properties of binder materials

Characteristics	GBFS	FA	SF	QP
Chemical component				
SiO ₂	37.98	59.45	98.90	97.88
Al_2O_3	12.55	21.42	0.25	0.26
Fe ₂ O ₃	1.51	5.91	0.13	0.15
CaO	39.95	6.73	0.27	0.2
SO ₃	2.69	0.15	_	1.51
Na_2O	0.76	1.50	0.17	_
K ₂ O	0.70	1.66	0.12	_
MgO	3.86	1.78	0.16	_
TiO ₂	_	1.40	_	_
Physical characteristics				
Specific surface area (cm ² ·g ⁻¹)	6,175	6,840	19,750	4,085
Specific gravity	2.55	2.34	2.15	2.58

2.1.2 FA

FA is a residual material produced by coal-fired power stations. It is categorized as class F FA based on the specifications outlined in ASTM C618 Class F [35]. The earlier studies [36,37] established a constant concentration of 270 kg·m⁻³ for FA. The characteristics of the utilized FA are presented in Table 1.

2.1.3 SF

SF was obtained from Sika Company, and it is in accordance with ASTM C1240 standards [38]. SF can be defined as a by-product of ferrosilicon alloy production and was used as a pozzolanic effect [39-41]. The physical and chemical properties of SF are tabulated in Table 1.

In conclusion, Table 1 shows the chemical composition of binder materials used in this study to show the materials components that have a vital role in reactions hence concrete performance. Results were obtained via performing XRF X-ray fluorescence on small samples, then compressed, and heated for testing.

2.1.4 NM

This study used two types of NM: NS with 99.5% SiO₂ and NT with 99.0% TiO₂. The NM (NS and NT) was synthesized in the science laboratory of Beni Suef University, Egypt. In comparison, NS or NT was added at nine contents: 0, 0.5, 1.0, 1.5, 2.0, 2.5, 3.0, 3.5, and 4.0% by weight of binder materials (GBFS and FA and SF) [28,42,43]. Table 2 summarizes the physical characteristics of NM provided by the manufacturer.

Table 2: Properties of NM

Properties	NS	NT		
Form	Powder	Powder		
Boiling point	2,230°C	2,500-3,000°C		
Formula	99.5% SiO ₂	99% TiO ₂		
Density	2.2–2.6 g·cm ⁻³	3.79 g·cm ^{−3}		
Color	White	White		
Particle size	20 ± 5 nm	5 nm		
Water solubility	Insoluble	Insoluble		
Melting point	1,600°C	1,825°C		
Molecular weight	60.08 g·mol ^{−1}	79.88 g·mol ^{−1}		
Specific gravity	2.2	3.85		

2.1.5 St.F

St.F at a constant content of 1% in terms of volume were used to reinforce the UHPGC mixes, based on the previous work [30,44,45]. The St.F used in this study was obtained from Hany Mahros Steel Fiber, Kaluob, Egypt. St.F properties from the source (manufacturing company) are shown in Table 3.

2.1.6 Quartz powder (QP)

The filler utilized in this article is OP with an average particle size of approximately between 10 and 25 µm [46,47]. The characteristics of OP are displayed in Table 4.

2.1.7 Quartz sand

To enhance the uniformity of the fine aggregate, quartz sand was utilized as a fine aggregate, and its average particle size was decreased to 4.75 mm. All mixtures in this study are based on 100% fine aggregate [48]. The properties of the fine aggregate were evaluated according to the requirements of ASTM C33/C33M-18 [49]. The physical properties and the

Table 3: Properties of St.F

St.F	
Diameter (mm)	0.12
Length (mm)	12
Aspect (ratio)	100
Density (kg·m ⁻³)	7,800
Elastic modulus (GPa)	194
Tensile strength (GPa)	1.82

Table 4: Properties of the QP

	Physical properties		Chemical compositions (%)						
Colour	Specific area (cm²⋅g ⁻¹)	Specific gravity	SiO ₂	Al ₂ O ₃	Fe ₂ O ₃	CaO	SO ₃		
White	4,085	2.58	97.88	0.26	0.15	0.2	1.51		

Table 5: Properties of quartz sand

Specific gravity	Unit weight (kg·m ⁻³)	Fineness modulus	Water absorption (%)	Clay and fine materials (%)	
2.66	1,690	2.627	0.96	0.78	

grading curve of the fine aggregate are given in Table 5 and Figure 1, respectively.

2.1.8 Alkaline solutions

The alkaline activator solutions used were sodium hydroxide (NaOH) with a 98% purity and sodium silicate (Na₂SiO₃) composed of 34.42% SiO₂, 15.26% Na₂O, and 50.32% H₂O. The alkaline solution containing NaOH and Na₂SiO₃ was acquired from El-Epour City, Egypt. The concentration of NaOH remained constant at 16M based on the previous research to produce UHPGC [7,12,50–54], while the concentration of Na₂SiO₃ varied in the synthesis of the alkaline activator. To create a solution with the desired concentration, it is necessary to dissolve the solids in water. It is highly recommended to prepare the sodium hydroxide solution (SHS) at least 24 h before using

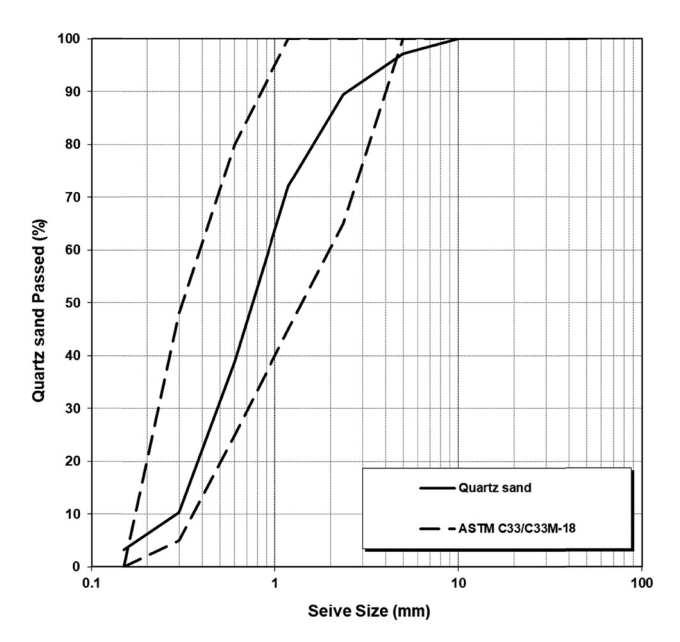


Figure 1: Grading curve of used quartz sand.

it. During the experimental work, a consistent alkaline liquid ratio of 1:3 (SHS:sodium silicate solution [SSS]) and an alkaline solution to binder materials ratio of 0.37 were utilized for all the mixes [55–57].

2.1.9 Superplasticizer (SP)

A high-range water-reducing additive, SP (Viscocrete-5930), was used to enhance the workability of UHPGC. The material meets specifications for ASTM-C-494 Types G and F, with a specific gravity of 1.09 [58]. The materials used in this study are seen in Figure 2.

2.2 Mix ratios and mixing procedure

This study investigated the effect of adding NM to UHPGC mixtures. Three groups of 17 mixtures were examined, with the first group acting as a control mixture without any NM. The second set of mix ratios was examined, consisting of eight distinct mixes with varying NS contents (0.5, 1.0, 1.5, 2.0, 2.5, 3.0, 3.5, and 4.0%) by weight of binder materials to produce UHPGC. The third group is the same as the second group, except it uses NT with identical content. The mix design for UHPGC included constant proportions of 730 kg·m $^{-3}$ GBFS, 270 kg·m $^{-3}$ FA, 150 kg·m $^{-3}$ SF, and 200 kg·m $^{-3}$ QP. Table 6 shows different ratios of UHPGC mixtures, with a fixed proportion of 0.37 for the alkaline activator solution to the binder.

For this study, an axial mixer was used to uniformly mix UHPGC, which was poured into molds to create specimens. The mix contained sodium hydroxide flakes, SSS, and a blend of dry components, including binder materials (GBFS, FA, SF), QP, quartz sand, and St.F. The mixture was blended for 5 min in a blender and an additional 5 min in a mixer. The cured specimens were evaluated for age after being kept in an oven at 80°C for 48 h and then cured at room temperature.



Figure 2: Materials used in this study.

2.3 Test procedure

NM compositions' impact on the workability of UHPGC composites was evaluated using ASTM-C-143-15a for flow diameter. The compression test of the cubic UHPGC specimens measuring $100~\text{mm} \times 100~\text{mm} \times 100~\text{mm}$ was

measured at 3, 7, 28, and 90 days following the guidelines of BS-1881:part-116-2004. For each test period, we averaged three specimens. All specimens were tested in a hydraulic testing machine with a capacity of 200 tons and an accuracy of 0.5 tons. The CS " $f_{\rm c}$ " was calculated using the formula:

Table 6: Mix proportions for UHPGC mixtures

Mixtures ID	GBFS	FA	SF	NS	NT	St.F	QP	Sand	SHS		SSS	AS/MA	SP
	kg·m ^{−3}	kg·m ^{−3}	kg·m ^{−3}	%	%	%	kg·m ^{−3}	%	Ratio	Mol.	Ratio	Ratio	%
Control	730	270	150	0	0	1.0	200	100	1	16	3	0.37	1.5
NS 0.5	730	270	150	0.5	0	1.0	200	100	1	16	3	0.37	1.5
NS 1.0	730	270	150	1.0	0	1.0	200	100	1	16	3	0.37	1.5
NS 1.5	730	270	150	1.5	0	1.0	200	100	1	16	3	0.37	1.5
NS 2.0	730	270	150	2.0	0	1.0	200	100	1	16	3	0.37	1.5
NS 2.5	730	270	150	2.5	0	1.0	200	100	1	16	3	0.37	1.5
NS 3.0	730	270	150	3.0	0	1.0	200	100	1	16	3	0.37	1.5
NS 3.5	730	270	150	3.5	0	1.0	200	100	1	16	3	0.37	1.5
NS 4.0	730	270	150	4.0	0	1.0	200	100	1	16	3	0.37	1.5
NT 0.5	730	270	150	0	0.5	1.0	200	100	1	16	3	0.37	1.5
NT 1.0	730	270	150	0	1.0	1.0	200	100	1	16	3	0.37	1.5
NT 1.5	730	270	150	0	1.5	1.0	200	100	1	16	3	0.37	1.5
NT 2.0	730	270	150	0	2.0	1.0	200	100	1	16	3	0.37	1.5
NT 2.5	730	270	150	0	2.5	1.0	200	100	1	16	3	0.37	1.5
NT 3.0	730	270	150	0	3.0	1.0	200	100	1	16	3	0.37	1.5
NT 3.5	730	270	150	0	3.5	1.0	200	100	1	16	3	0.37	1.5
NT 4.0	730	270	150	0	4.0	1.0	200	100	1	16	3	0.37	1.5

SHS is a sodium hydroxide solution.

SSS is a sodium silicate solution.

Mol. is a molarity.

AS/MA is an alkaline solution to mineral additives.

SP is a superplasticizer.

where P_c is the maximum load in compression and A is the cross-sectional area of the specimen.

The water permeability (WP) test was conducted on cylindrical specimens of 150 mm \times 150 mm at 28 days, according to BS EN 12390-8 [59]. 100 mm diameter and 50 mm thickness disk specimens were tested for chloride penetration (CP) test using the ASTM C1202-17 [60] procedure. The water sorptivity (WS) test at 28 days measures the water absorption rate according to ASTM C1585-13 [61] on a 100 mm \times 50 mm cylinder. To assess sulfate resistance in specimens, follow ASTM C1012 [62]. Add 0–100 g·L⁻¹ sodium sulfate solution to a water pool. Test 70 mm \times 70 mm \times 70 mm specimens for CS at 28, 90, and 180 days to investigate short-, medium-, and long-term impacts. The testing procedure in this study is seen in Figure 3.

3 Results and discussion

3.1 Fresh properties

Figure 4 shows how the slump flow of UHPGC is affected by NS and NT concentration. The focus was on replacement ratios ranging from 0.5 to 4%. An unfavorable correlation was observed with the increasing ratio of NS usage. NS reduces slump flow due to its interaction with the geopolymer matrix, resulting in a gradual decrease from 544 to 450 mm. An increase in the replacement ratio of NS is likely

to enhance the reactivity and bonding with alkali-activated geopolymer gel due to its large surface area and pozzolanic properties [20,63]. The increased contact between the components results in a less flexible and more compact geopolymer structure. This causes a reduction in the slump flow, indicating decreased ease of handling.

This study investigates the impact of NT on the slump flow of UHPGC at different replacement ratios ranging from 0.5 to 4%. The concentration of NT increased and caused a corresponding reduction in the slump flow, which is a crucial measure of the workability of concrete, as demonstrated by a clear pattern of decline. The observed behavior can be explained by the distinct interactions between the nano-titanium and the geopolymer matrix. The addition of 4% NT is expected to increase the viscosity and decrease the flowability of UHPGC, resulting in a decrease from 544 to 470 in the rheological characteristics compared to the control mix. The addition of NT, which has pozzolanic and cementitious properties, may improve the formation of more compact and less pliable geopolymer structures [23,64,65]. The decrease in slump flow highlights the importance of understanding the role of NT in UHPGC mixtures.

3.2 CS

Figures 5 and 6 show the CS of UHPGC containing NS and NT by 0, 0.5, 1.0, 1.5, 2.0, 2.5, 3.0, 3.5, and 4.0% of binder materials, at test ages of 3, 7, 28, 90, and 180 days. The use of



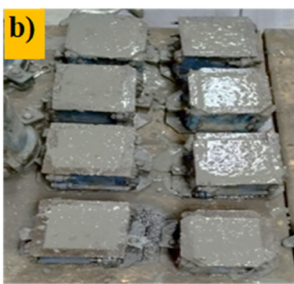








Figure 3: Testing procedure in this study: (a) slump flow test, (b) concrete samples, (c) compression test, and (d) WP.

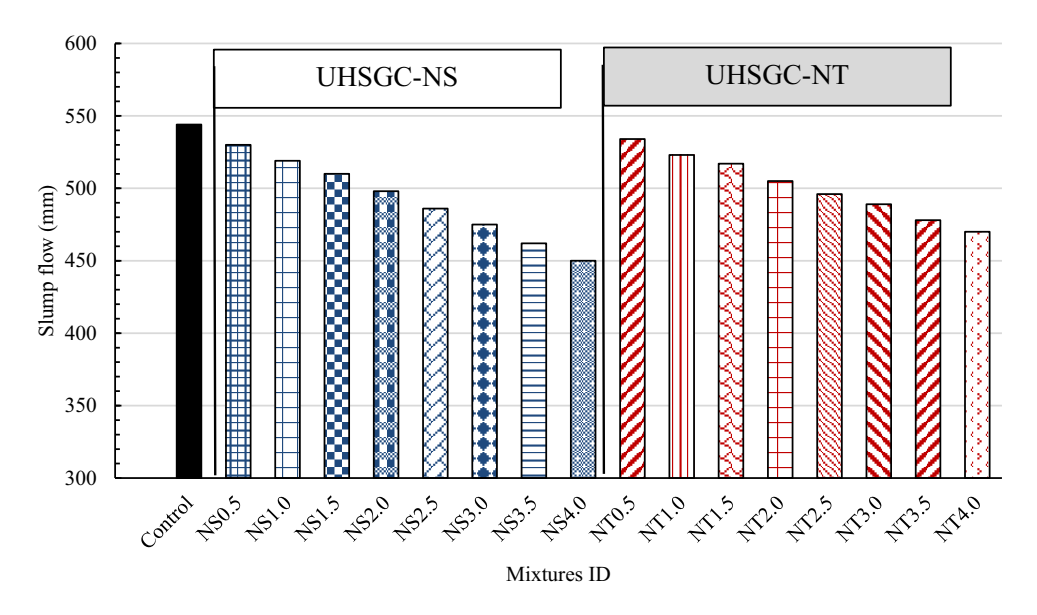


Figure 4: Slump flow of UHPGC incorporating NS and NT.

NS improved the strength properties of UHPGC. Therefore, the CS of UHPGC was 150.8, 159.7, 169.0, 177.9, 188.6, 198.7, 183.5, 175.7, and 171.9 MPa at 28 days of test age, with the addition of 0, 0.5, 1.0, 1.5, 2.0, 2.5, 3.0, 3.5, and 4.0% of NS, respectively. It is also noted that the highest CS was achieved for the mixture NS 2.5 when adding 2.5% of NS. It was the CS of 161.0, 176.8, 198.7, 217.0, and 222.2 MPa for ages test 3, 7, 28, 90, and 180 days, respectively. Accordingly, increasing the addition percentage of NS contributed

to improving the CS with an upward relationship from 0.5 to 2.5%, while the CS decreased at higher addition rates. However, all percentages of NS addition ranging from 0.5 to 4.0% resulted in higher CS compared to the reference mixture. Previous research indicates the incorporation of NM, in particular NS, contributed to the improvement in CS when compared to geopolymer-free nanostructured materials. It is possible that the enhanced strength of UHPGC is a result of the presence of NS, which may fill the nanopores

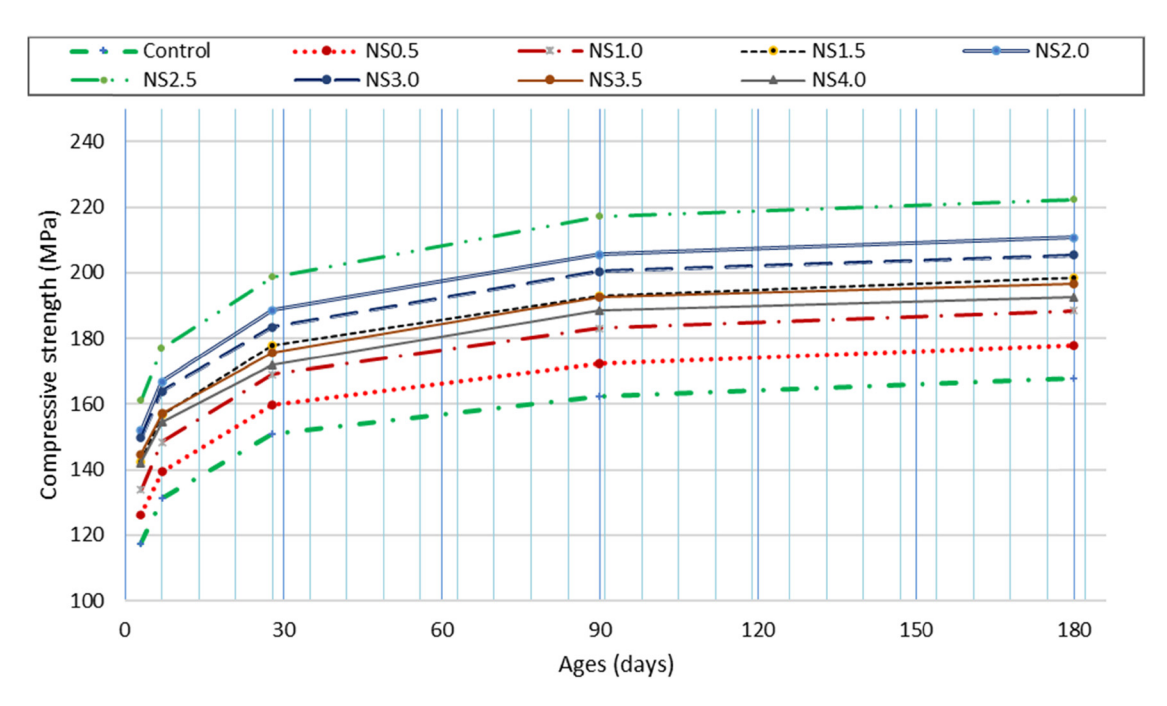


Figure 5: Results of CS test of UHPGC containing NS.

8 — Abdullah M. Zeyad *et al.* DE GRUYTER

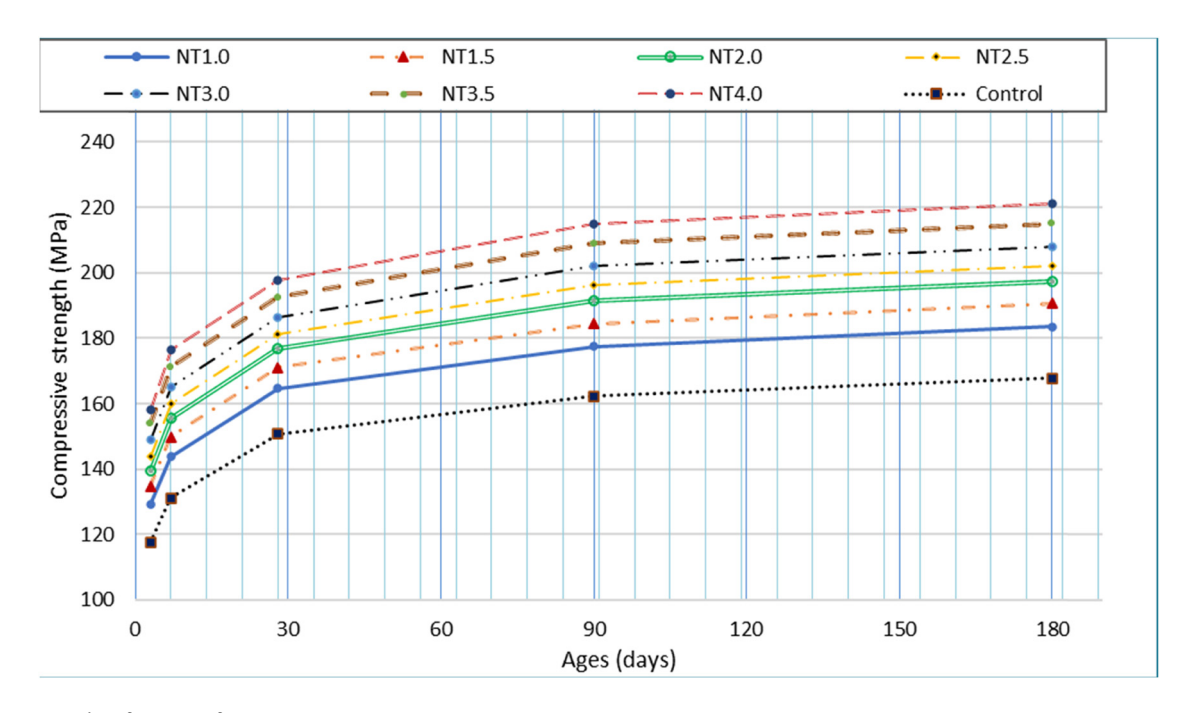


Figure 6: Results of CS test of UHPGC containing NT.

within the geopolymer matrix, producing a more densely packed matrix. Furthermore, it has been observed that the chemical properties of silica-rich NS have a significant impact on the acceleration of geopolymer reactions, resulting in a stronger geopolymer matrix and ultimately leading to enhanced sample strength. In previous studies, researchers have found that the optimal amount of NS content to improve the CS is between 1.0 and 4.0%. However, it was observed that after this dose, there was a slight reduction in CS due to the flooding in the un-interacted NS particle matrix. The optimal rate of NS incorporation to enhance CS is 2.5%, as indicated by the findings of this study. Consequently, the slight reduction in CS that occurs when the concentration of NS exceeds 2.5% may be attributed to the presence of unreacted NS particles in the matrix. Consequently, the agglomeration of NS particles between themselves prevents the dissolution of silica and leads to the formation of voids, thereby reducing the CS of geopolymer concrete. Nuaklong et al. discovered that a slight decrease in CS occurred when the concentration of NS exceeded 2% [66]. This, in turn, led to the formation of voids and a subsequent decrease in the CS of GC. In previous studies conducted by researchers [66–68], it was found that the CS of GC can be enhanced by the addition of NS. These studies revealed that a specific dose of NS can lead to an increase in CS. According to the findings of Nuaklong et al. [66], the addition of NS has been shown to enhance the CS of GC by approximately 2%.

The inclusion of NS primarily impacts the dissolution phase of geopolymerization, potentially leading to an

improvement in the rate of geopolymerization. It appears that the inclusion of NS has a positive impact on the production of reaction products and the degree of geopolymerization, leading to a more consistent and condensed matrix [69]. The results also illustrate that the addition of NT to the UHPGC contributed to the improvement of the CS of the concrete at all rates of addition (0.5, 1.0, 1.5, 2.0, 2.5, 3.0, 3.5, 4.0% NT) for all test ages compared to the reference mixture. The results showed that a higher rate of NT addition led to an increase in the CS. The mixture NT4.0 which includes an addition rate of 4% NT achieved the highest CS among the mixtures containing NT. The CS was from 158.3, 176.4, 97.6, 214.8, 215.0, and MPa at test ages 3, 7, 28, 90, and 180 days, respectively. The observed increase in CS can be attributed to the beneficial effects of NT in the microstructure. These effects include the filling of nanopores within the geopolymer matrix, in addition to promoting nucleation during fermentation (crystal nucleus effect or seeding effect), resulting in a more uniform distribution of hydration products [23]. This is consistent with the statement of Sanalkumar and Yang that the addition of 1-10% NT leads to an enhancement of the CS of GC mixtures [70].

3.3 Microstructure

SEM micrographs of three UHPGC mixes, control, NS 2.5, and NT 4, are shown in Figure 7a–c, respectively. The addition of 2.5% NS to UHPGC significantly alters its microstructure. The

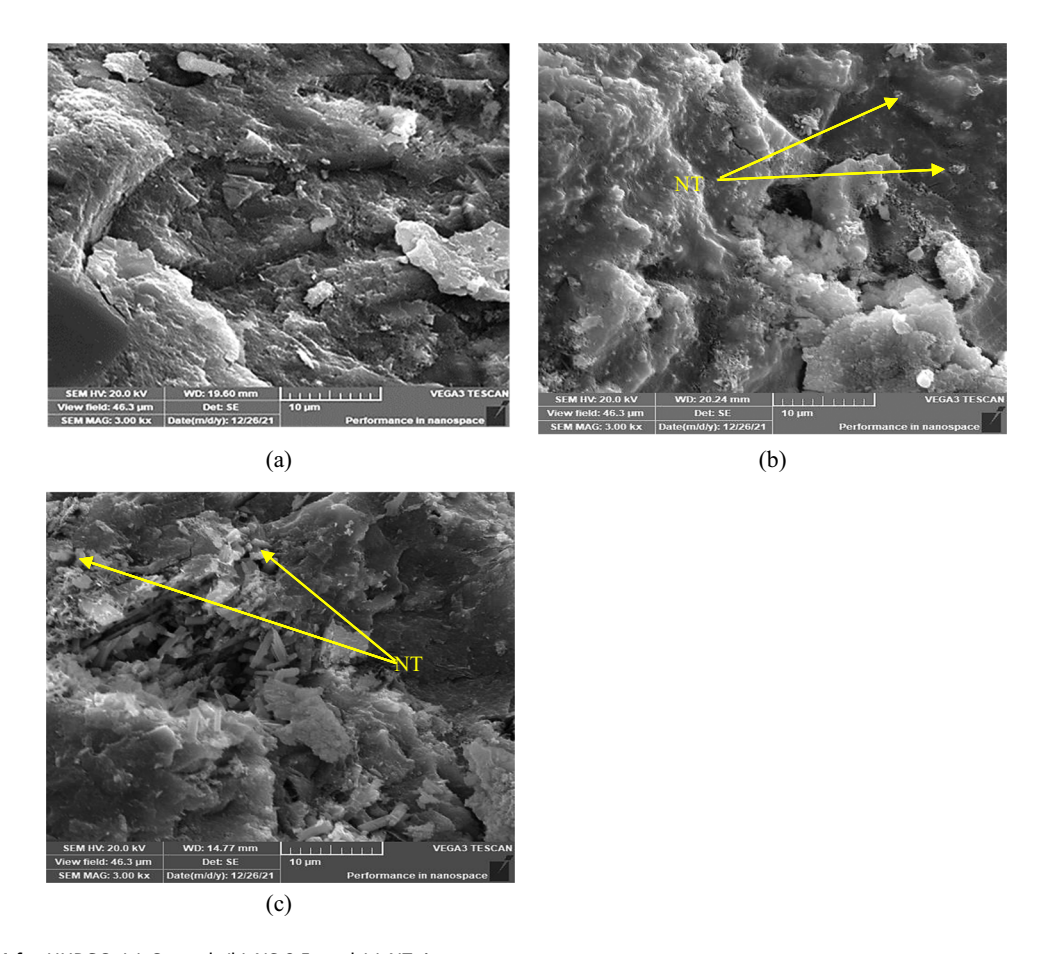


Figure 7: SEM for UHPGC. (a) Control, (b) NS 2.5, and (c) NT 4.

use of NS particles improves the geopolymer matrix due to its large surface area and pozzolanic properties. A study using SEM showed that the resulting microstructure is denser and more compact, with lower porosity and improved bonding between the geopolymer gel and the aggregates. The addition of 2.5% NS to UHPGC facilitates the creation of additional reaction products. This leads to an improvement in the overall crystalline structure, resulting in enhanced CS, transport properties, and SA. As a result, UHPGC with 2.5% NS is a highly promising option for high-performance construction applications [24]. In contrast, the microstructure of UHPGC containing 4% NT exhibits different alterations compared to the version without nano-additions A distinct morphology was observed in the SEM images, with evenly dispersed nanoscale titanium particles within the geopolymeric matrix. The addition of NT improved the microstructure, resulting in a more uniform distribution of the particles. As a result of this modification, there was an increase in the bonding between the interfaces and a higher packing density [71]. This led to improved strength and endurance. When using larger replacement ratios, such as 4%, it is important to consider the possibility of agglomeration effects. An analysis of the microstructure

reveals the complex function of nano-additives in enhancing the internal structure of UHPGC. Therefore, careful incorporation of these additives is necessary to achieve exceptional material performance [72]. Comparative evaluations have shown that the changes in the microstructure caused by the addition of 4% nano-additives have a beneficial impact on the mechanical [73] and durability characteristics of UHPGC [74], providing valuable information for the development and use of sophisticated construction materials.

3.4 Transport properties

3.4.1 WP

The findings from the WP test on UHPGC samples after 28 days are shown in Figure 8. Overall, the study indicates that the WP values of the UHPGC samples varied between 0.90 and $1.38 \times 10^{-11} \ \mathrm{cm} \cdot \mathrm{s}^{-1}$ for mixtures that included NS. The study's findings indicate that the WP values for UHPGC samples varied between 0.85 and $1.43 \times 10^{-11} \ \mathrm{cm} \cdot \mathrm{s}^{-1}$ when mixed with NT. The control mixture lacking NM (NS and

NT) had a WP value of $1.55 \times 10^{-11} \,\mathrm{cm \cdot s^{-1}}$, as observed during the study. The results show that the inclusion of NS in UHPGC production significantly reduced the WP values compared to the reference mixture, and the results were 1.38, 1.27, 1.18, 1.10, 1.04, 1.0, 0.95, and 0.90×10^{-11} cm·s⁻¹ for the NS 0.5, NS 1.0, NS 1.5, NS 2.0, NS 2.5, NS 3.0, NS 3.5, and NS 4.0, respectively. According to the observation, the addition of nanoparticles has resulted in better resistance to permeability in UHPGC. The improvement in resistance was noted with an increase in the rate of addition. This finding is consistent with many other previous studies that have confirmed the crucial role of NM in filling micropores and increasing the density of the geopolymer paste matrix [69,75]. The incorporation of NS led to a positive impact on the porosity and pore structure of the matrix by reducing the number of macropores [76]. The findings indicate that the incorporation of NS in the production of UHPGC led to a significant reduction in WP values in comparison to the reference mixture. The recorded values were 1.43, 1.32, 1.23, 1.14, 1.07, 0.98, 0.92, and 0.85×10^{-11} cm·s⁻¹ for the NT0.5, NT 1.0, NT 1.5, NT 2.0, NT 2.5, NT 3.0, NT 3.5, and NT 4.0, respectively. This observation indicates that the incorporation of NT resulted in an enhancement of the UHPGC's impermeability resistance, which was proportional to the rate of addition. This is attributed to the role of NM in reducing the size of the pores, closing them, or cutting the pathways connected to them, which prevents or reduces the WP through the geopolymer paste. The results obtained from this study support the theory of previous research, which confirms the

positive role of adding nanoparticles to concrete to achieve lower permeability and higher durability [64,77].

3.4.2 CP

Figure 9 shows the results of the CP test for UHPGC samples at a test age of 28 days. It is noticeable that the CP of UHPGC samples that contain NM is improved. The CP values for UHPGC samples that contained NS ranged between 138 and 260 (Columb). While the CP test results for UHPGC samples that included NT were between 272 and 130 (Columb). As for the control mixture without NM (NS and NT), the CP value was 340 (Columb). Accordingly, the NT4.0 mixture achieved the lowest chloride permeability at 130 (Columb), followed by the NS4.0 mixture with a permeability value of 138 (Columb). Based on the results presented, it can be concluded that incorporating nanoparticles in concrete improves its impermeability. As the rate of addition of NM increases, the permeability of concrete decreases gradually. This is due to the ability of NM to enhance the polymerization process and reduce pore size [23,78].

3.4.3 WS

The data presented in Figure 10 display the WS coefficient values for UHPGC samples after 28 days of testing. Based on the findings, it appears that the inclusion of NM (NS or NT) in UHPGC samples led to a reduction in the WS coefficient

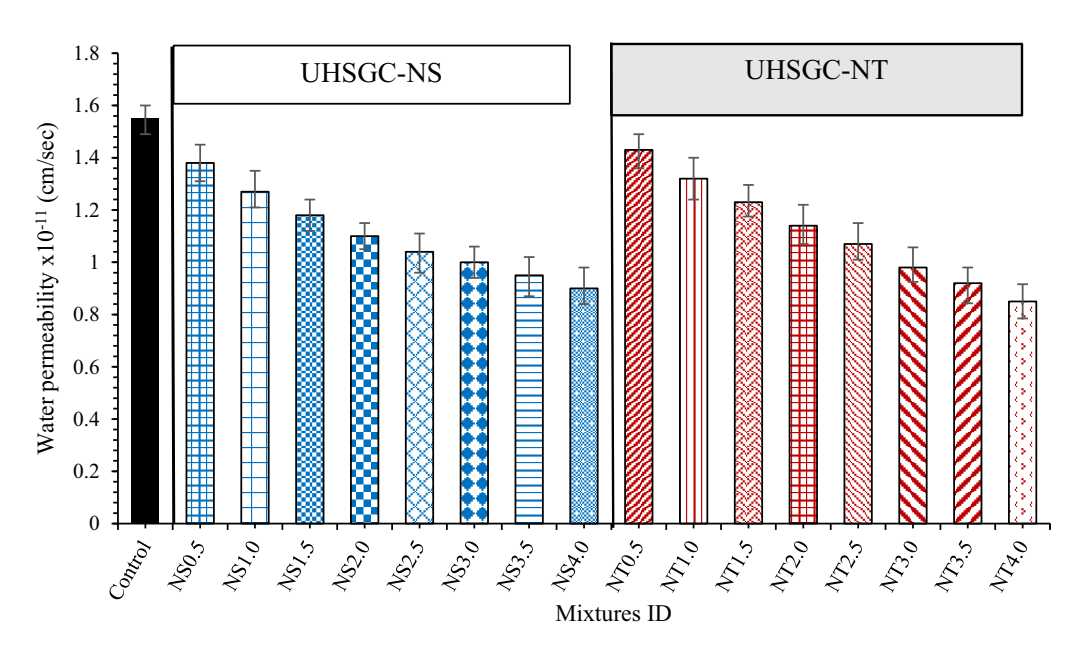


Figure 8: Results of WP test of UHPGC containing NS and NT.

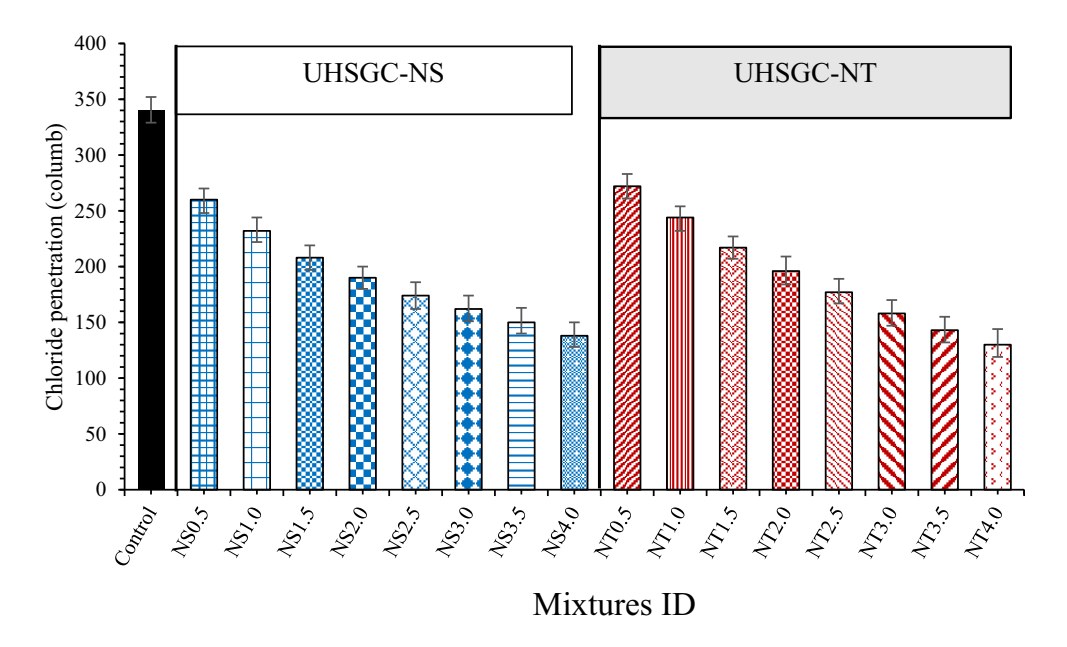


Figure 9: Results of CP test of UHPGC containing NS and NT.

values. The WS coefficient values for UHPGC samples containing NS were observed to range between 2.4 and 1.28 (10⁻⁴ mm·s⁻¹ 0.5). The WS coefficient values for UHPGC samples containing NT ranged from 2.55 to 1.20 (10⁻⁴ mm·s⁻¹ 0.5). In the case of the control mixture without NS and NT, the WS coefficient was measured to be 2.95 (10⁻⁴ mm·s⁻¹ 0.5). Based on the results, it appears that the NT4.0 mixture demonstrated the most favorable WS coefficient value of 1.20 (10⁻⁴ mm·s⁻¹ 0.5), while the NS4.0 mixture exhibited a slightly higher water diffusion coefficient value of 1.28

(10⁻⁴ mm·s⁻¹ 0.5). Based on the findings presented it appears that the inclusion of nanoparticles has a positive impact on the impermeability of concrete. The results show a clear correlation between the increase in the rate of addition of NM and the gradual decrease in the water absorption coefficient. This may be attributed to the role played by NM in enhancing the polymerization process and reducing pore size [23,78].

According to previous studies, it has been suggested that geopolymer mixtures incorporating FA and GBFS with

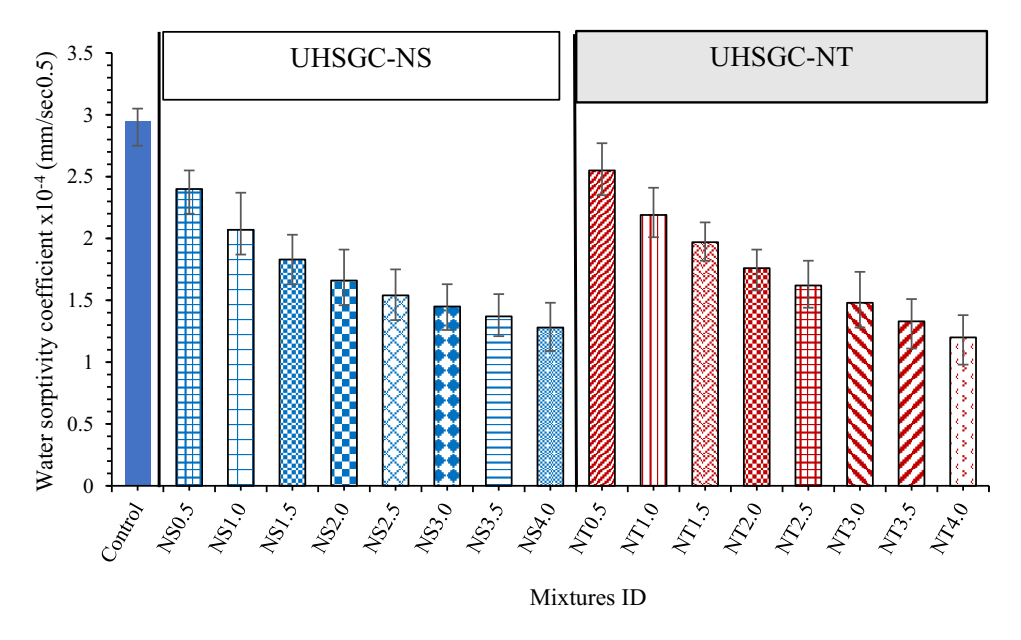


Figure 10: Results of WS test of UHPGC containing NS and NT.

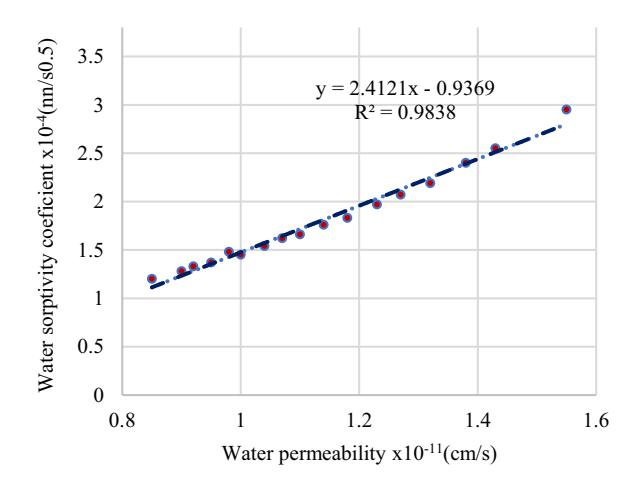
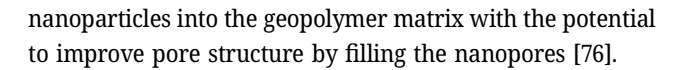


Figure 11: Relationship between WP and WS of UHPGC.

NS or NT can enhance the characteristics of GC, subject to the addition rate. The effectiveness of the added NM to geopolymer mixtures is contingent upon their chemical composition and fineness [64,77,78]. Based on the available results, it appears that the findings of previous researchers regarding the mechanism of action of NM can be supported. These findings suggest that NM tends to concentrate on three specific points. This study primarily focuses on the framework of NM (NS and NT) on UHPGC. The unique properties of nanoparticles, such as (1) the effect of small particle size, significant surface area, and high surface energy have a significant impact on the potential impact of NM on the geopolymer matrix [69]. (2) The phenomenon of nucleation, the nanoparticles have a significant surface area and surface energy, which serve as a nucleation for a less porous geopolymer matrix. This, in turn, causes the geopolymerization process to accelerate [63]. (3) The effect of nanopore filling, which is the incorporation of



3.4.4 Relationship between the transport properties of UHPGC

Transport properties such as CP, WP, and WS in UHPGCembedded NM have a strong correlation because they are all influenced by the same factors. The permeability of UHPGC is primarily determined by the pores, their diffusion, their connectivity, and their continuity within the microstructure. In this study, the hypothesis that transport characteristics are interrelated was confirmed, and a relationship was established that demonstrated the validity of tests conducted on UHPGC at 28 days of age. Figures 11-13 illustrate the results, which indicate that there is a significant correlation between WP and WS, as indicated by a correlation coefficient of $R^2 = 0.99$; a significant correlation coefficient between WS and CP, as indicated by a correlation coefficient of $R^2 = 0.99$; and a significant correlation between WP and CP, as indicated by a correlation coefficient of R^2 = 0.97. A correlation coefficient, R, demonstrates that these findings are related. In addition, it is stated that all correlation coefficients are exceedingly high, exceeding $(R^2 = 0.97)$ with regard to the transport properties of UHPGC. Due to the exceedingly high correlation between the transport properties of UHPC and UHPGC, it appears that concrete samples with high robustness also have low WP. The low WP indicates the effectiveness of preventing the penetration of chloride ions, whose diffusion within concrete can result in corrosion of the steel reinforcement. In addition, the reduction in WP exacerbates the reduction in the rise of gases and liquids within the concrete, thereby

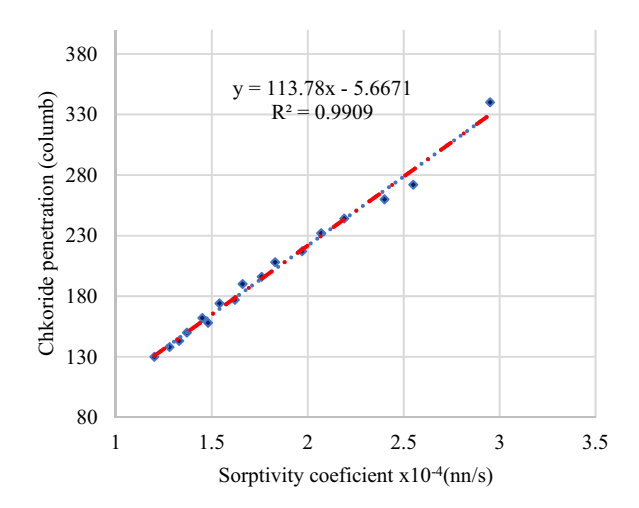


Figure 12: Relationship between WS and CP of UHPGC.

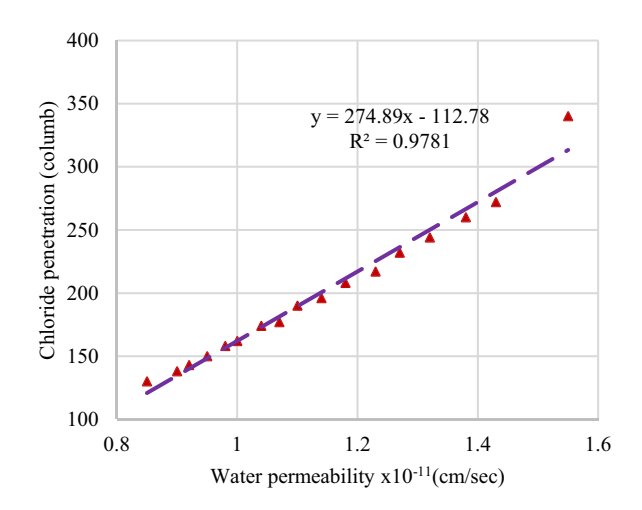


Figure 13: Relationship between WP and CP of UHPGC.

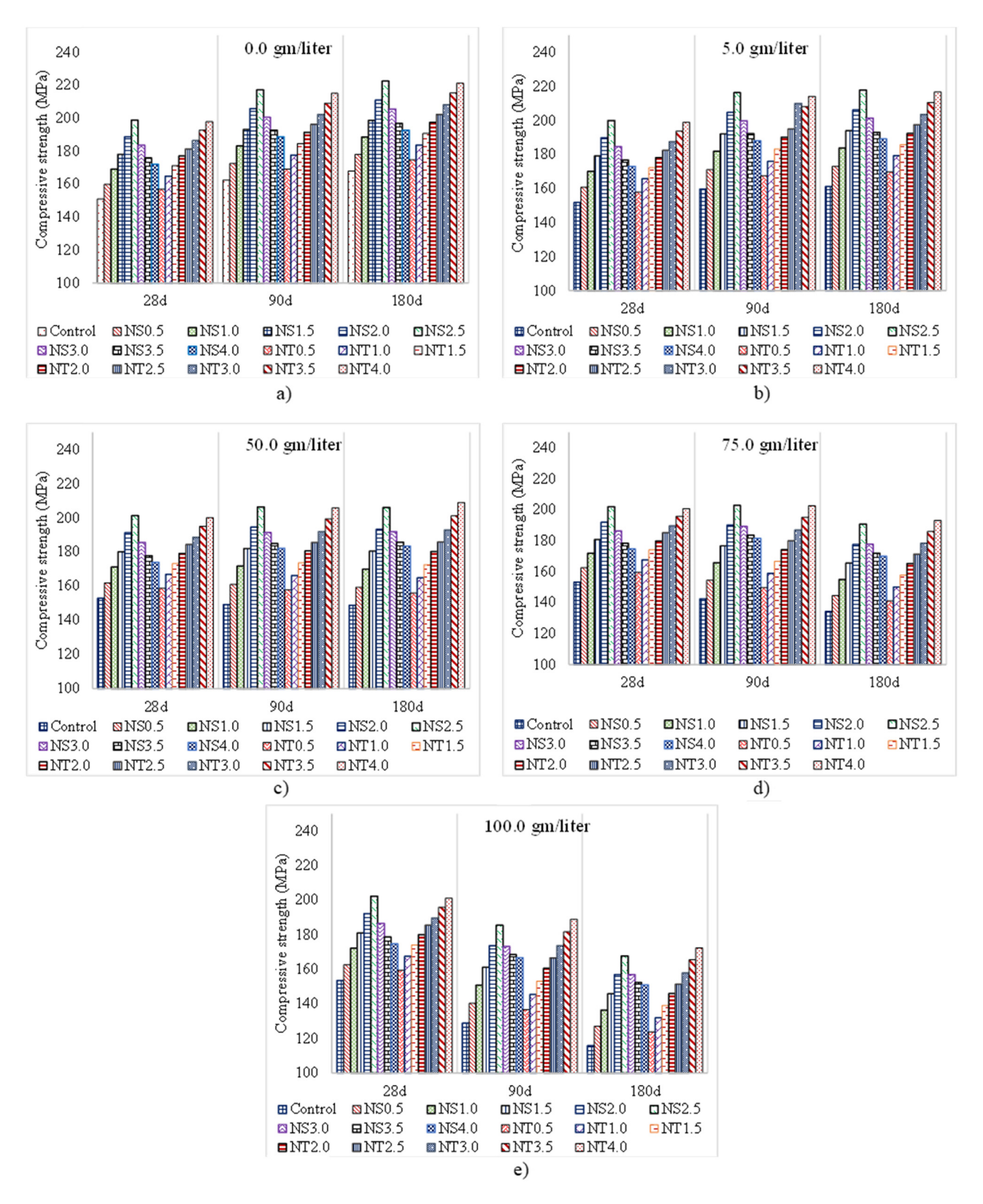


Figure 14: SA (Na₂SO₄) of UHPGC. (a) Concentrations of sodium sulfate of no attack. (b) Concentrations of sodium sulfate of low attack. (c) Concentrations of sodium sulfate of medium attack. (d) Concentrations of sodium sulfate of high attack. (e) Concentrations of sodium sulfate of severe attack.

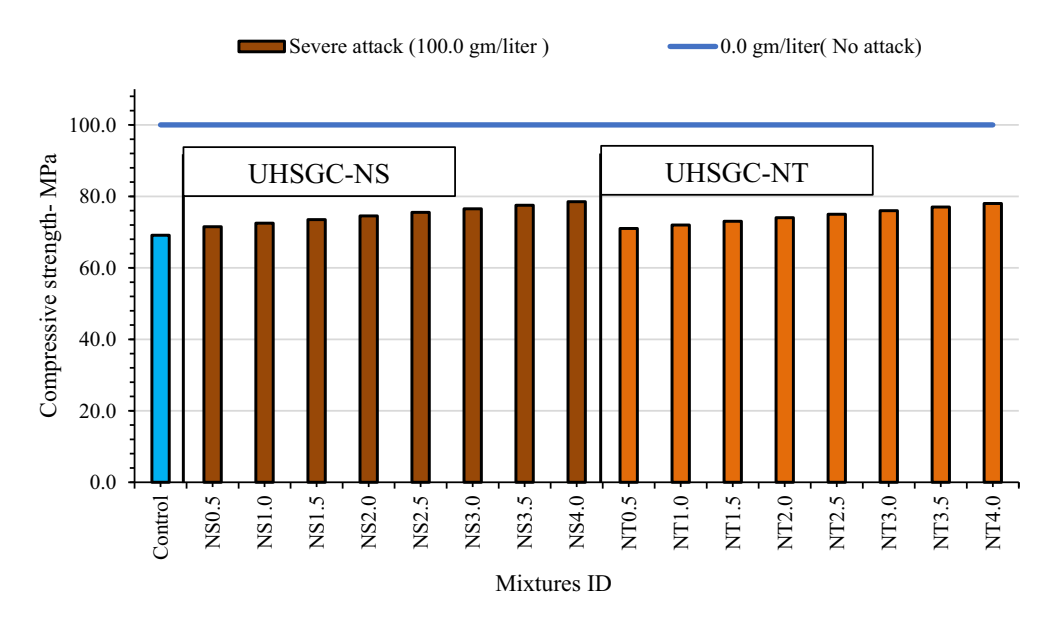


Figure 15: Residual CS after exposure of concrete to the concentration of sodium sulfate of 100 q·L⁻¹ for 180 days.

reducing concrete deterioration over time. Several studies in the past have confirmed the existence of a significant correlation between the conveyance properties of concrete [79–81].

3.5 SA

The results of SA (Na₂SO₄) on UHPGC at varying concentrations of $0.0-100.0 \text{ g}\cdot\text{L}^{-1}$ over a period of 28, 90, and 180 days are shown in Figure 14a-e. Figure 14a illustrates the CS of no SA of UHPGC, where 0.0 mg·L⁻¹ (no attack) is the reference mixture for calculating a loss in CS upon SA exposure. As shown in Figure 14b, the CS of UHPGC was not significantly affected by SA at concentrations as low as 5 mg·L⁻¹ (low attack) over a period of 180 days. The reduction in CS was between 1.7 and 3.9% of the CS without SA. In addition, it can be seen in Figure 14c and d that the CS decreased more rapidly when SA exposure at the concentration was increased by 50 mg·L⁻¹ (medium attack) and 75 mg·L⁻¹ (high attack) over a period of 180 days. When subjected to SA at a concentration of 50 mg·L⁻¹, the decrease in CS of UHPGC ranged from 4.6 to 11.3% compared to the reference mixture, while the decrease in CS ranged from 11.8 to 20.0% of UHPGC upon exposure to a concentration of 75 mg·L⁻¹. Moreover, Figure 14e shows a significant decrease in the CS of the UHPGC samples subjected to 100 mg·L⁻¹ SA (extreme attack). This decrease in CS due to SA is most pronounced at an advanced age of 180 days. The decrease in CS of UHPGC ranges from 21.5 to 30.8% of the CS before SA. According to a previous study conducted by Bakharev et al. [82], it has been suggested that GC exhibits superior performance in sodium and magnesium sulfate environments compared to Portland cement concrete. Moreover, the incorporation of NM into GC has had a positive effect. According to the findings, UHPGCs that included NS or NT demonstrated superior efficacy in comparison to the control mixture [83].

Figure 15 illustrates the deterioration in concrete's CS after being exposed to Na_2SO_4 attack for 180 days. The results show that the lowest loss in CS was from half of the mixture NS4.0 and NT4.0 by the amount of retention of 78.5 and 78%, respectively.

4 Conclusions

This study aims to assess the effectiveness of UHPGC by analyzing its properties with varying amounts of NS and NT. The research examines how different concentrations affect key parameters such as CS, transport properties, and resistance to SA. After analyzing the data presented in this study, the following conclusions can be drawn:

- Gradual decreases in slump flow diameter were observed for cement additions with NS and NT, with reductions of 17 and 13%, respectively.
- Adding 2.5% of NS to the mixture NS2.5 resulted in the highest CS of 161.0, 176.8, 198.7, 217.0, and 222.2 MPa for ages 3, 7, 28, 90, and 180 days, respectively.
- The CS of 4% NT mix was recorded as 158.3, 176.4, 97.6, 214.8, and 215.0 MPa at test ages of 3, 7, 28, 90, and 180 days, respectively.

- The higher the adding dosage of NS or NT, the lower the WS, with reductions up to 59% in the case of NS and 61.7% in the case of NT.
- NS and NT facilitate the formation of additional reaction products, thereby enhancing the overall crystalline structure. The improved microstructure is correlated with superior mechanical properties.
- CP test results for UHPGC samples that included NT were between 272 and 130 (Columb). As for the control mixture without NM (NS and NT), the CP value was 340 (Columb). Accordingly, the NT4.0 mixture achieved the lowest chloride permeability at 130 (Columb),
- · Significant decrease in the CS of the UHPGC samples subjected to 100 mg·L⁻¹ SA (extreme attack). This decrease in CS due to SA is most pronounced at an advanced age of 180 days. The decrease in CS of UHPGC ranges from 21.5 to 30.8% of the CS before SA.

5 Recommendations for future work

The performance of UHPGC in the presence of different NMs also in different durability investigations such as CP SA, corrosion, and elevated temperature needed to be performed.

Acknowledgments: The authors are thankful to the Deanship of Graduate Studies and Scientific Research at the University of Bisha for supporting this work through the Fast-Track Research Support Program.

Funding information: This work was supported by the Deanship of Graduate Studies and Scientific Research at the University of Bisha through the Fast-Track Research Support Program.

Author contributions: All authors have accepted responsibility for the entire content of this manuscript and approved its submission.

Conflict of interest: The authors state no conflict of interest.

Data availability statement: All data generated or analyzed during this study are included in this published article.

References

- Nurruddin, M. F., H. Sani, B. S. Mohammed, and I. Shaaban. Methods of curing geopolymer concrete: A review. International Journal of Advanced and Applied Sciences, Vol. 5, No. 1, 2018, pp. 31-36.
- [2] Ma, C. K., A. Z. Awang, and W. Omar. Structural and material performance of geopolymer concrete: A review. Construction and Building Materials, Vol. 186, 2018, pp. 90-102.
- Junior, J. A. L., A. R. G. de Azevedo, M. T. Marvila, S. R. Teixeira, R. Fediuk, and C. M. F. Vieira. Influence of processing parameters variation on the development of geopolymeric ceramic blocks with calcined kaolinite clay. Case Studies in Construction Materials, Vol. 16, 2022, id. e00897.
- Singh, B., G. Ishwarya, M. Gupta, and S. K. Bhattacharyya. Geopolymer concrete: A review of some recent developments. Construction and Building Materials, Vol. 85, 2015, pp. 78-90.
- [5] Li, C., H. Sun, and L. Li. A review: The comparison between alkaliactivated slag (Si + Ca) and metakaolin (Si + Al) cements. Cement and Concrete Research, Vol. 40, No. 9, 2010, pp. 1341-1349.
- Ranjbar, N., A. Kashefi, G. Ye, and M. Mehrali. Effects of heat and pressure on hot-pressed geopolymer. Construction and Building Materials, Vol. 231, 2020, id. 117106.
- Wetzel, A. and B. Middendorf. Influence of silica fume on properties of fresh and hardened ultra-high performance concrete based on alkali-activated slag. Cement and Concrete Composites, Vol. 100, 2019, pp. 53-59.
- Ambily, P. S., K. Ravisankar, C. Umarani, J. K. Dattatreya, and N. R. Iyer. Development of ultra-high-performance geopolymer concrete, Magazine of Concrete Research, Vol. 66, No. 2, 2014, pp. 82–89.
- [9] Lao, J. C., L. Y. Xu, B. T. Huang, J. X. Zhu, M. Khan, and J. G. Dai. Utilization of sodium carbonate activator in strain-hardening ultrahigh-performance geopolymer concrete (SH-UHPGC). Frontiers in Materials, Vol. 10, 2023, pp. 1-12.
- Ranjbar, N., M. Mehrali, M. R. Maheri, and M. Mehrali. Hot-pressed geopolymer. Cement and Concrete Research, Vol. 100, 2017, pp. 14-22.
- [11] Aydın, S. and B. Baradan. The effect of fiber properties on high performance alkali-activated slag/silica fume mortars. Composites Part B: Engineering, Vol. 45, No. 1, 2013, pp. 63-69.
- Liu, Y., C. Shi, Z. Zhang, N. Li, and D. Shi. Mechanical and fracture properties of ultra-high performance geopolymer concrete: Effects of steel fiber and silica fume. Cement and Concrete Composites, Vol. 112, 2020, id. 103665.
- Wu, Z., C. Shi, and K. H. Khayat. Investigation of mechanical properties and shrinkage of ultra-high performance concrete: Influence of steel fiber content and shape. Composites Part B: Engineering, Vol. 174, 2019, id. 107021.
- Yoo, D. Y., S. Kim, G. J. Park, J. J. Park, and S. W. Kim. Effects of fiber shape, aspect ratio, and volume fraction on flexural behavior of ultra-high-performance fiber-reinforced cement composites. Composite Structures, Vol. 174, 2017, pp. 375-388.
- Paruthi, S., A. Husain, P. Alam, A. H. Khan, M. A. Hasan, and H. M. Magbool. A review on material mix proportion and strength influence parameters of geopolymer concrete: Application of ANN model for GPC strength prediction. Construction and Building Materials, Vol. 356, 2022, id. 129253.

- [16] Shilar, F. A., S. V. Ganachari, V. B. Patil, T. M. Y. Khan, N. M. Almakayeel, and S. Alghamdi. Review on the relationship between nano modifications of geopolymer concrete and their structural characteristics. *Polymers*, Vol. 14, No. 7, 2022, id. 1421.
- [17] Verma, M. and N. Dev. Sodium hydroxide effect on the mechanical properties of flyash-slag based geopolymer concrete. *Structural Concrete*, Vol. 22, 2021, pp. E368–E379.
- [18] Niş, A., N. A. Eren, and A. Çevik. Effects of nanosilica and steel fibers on the impact resistance of slag based self-compacting alkali-activated concrete. *Ceramics International*, Vol. 47, No. 17, 2021, pp. 23905–23918.
- [19] Xu, Z., Q. Liu, H. Long, H. Deng, Z. Chen, and D. Hui. Influence of nano-SiO2 and steel fiber on mechanical and microstructural properties of red mud-based geopolymer concrete. *Construction and Building Materials*, Vol. 364, 2023, id. 129990.
- [20] Çevik, A., R. Alzeebaree, G. Humur, A. Niş, and M. E. Gülşan. Effect of nano-silica on the chemical durability and mechanical performance of fly ash based geopolymer concrete. *Ceramics International*, Vol. 44, No. 11, 2018, pp. 12253–12264.
- [21] Hakeem, I. Y., M. Alharthai, M. Amin, A. M. Zeyad, B. A. Tayeh, and I. S. Agwa. Properties of sustainable high-strength concrete containing large quantities of industrial wastes, nanosilica and recycled aggregates. *Journal of Materials Research and Technology*, Vol. 24, 2023, pp. 7444–7461.
- [22] Alomayri, T. Experimental study of the microstructural and mechanical properties of geopolymer paste with nano material (Al2O3). *Journal of Building Engineering*, Vol. 25, 2019, id. 100788.
- [23] Duan, P., C. Yan, W. Luo, and W. Zhou. Effects of adding nano-TiO₂ on compressive strength, drying shrinkage, carbonation and microstructure of fluidized bed fly ash based geopolymer paste. Construction and Building Materials, Vol. 106, 2016, pp. 115–125.
- [24] Ghanim, A. A. J., M. Amin, A. M. Zeyad, B. A. Tayeh, and I. S. Agwa. Effect of modified nano-titanium and fly ash on ultra-high-performance concrete properties. *Structural Concrete*, Vol. 24, No. 5, 2023, pp. 6815–6832.
- [25] Rawat, G., S. Gandhi, and Y. I. Murthy. Strength and rheological aspects of concrete containing nano-titanium dioxide. *Asian Journal* of Civil Engineering, Vol. 23, No. 8, 2022, pp. 1197–1208.
- [26] Assaedi, H., F. U. A. Shaikh, and I. M. Low. Characterizations of flax fabric reinforced nanoclay-geopolymer composites. *Composites Part B: Engineering*, Vol. 95, 2016, pp. 412–422.
- [27] Abbasi, S. M., H. Ahmadi, G. Khalaj, and B. Ghasemi. Microstructure and mechanical properties of a metakaolinite-based geopolymer nanocomposite reinforced with carbon nanotubes. *Ceramics International*, Vol. 42, No. 14, 2016, pp. 15171–15176.
- [28] Hakeem, I. Y., M. Amin, B. A. Abdelsalam, B. A. Tayeh, F. Althoey, and I. S. Agwa. Effects of nano-silica and micro-steel fiber on the engineering properties of ultra-high performance concrete. *Structural Engineering and Mechanics*, Vol. 82, No. 3, 2022, pp. 295–312.
- [29] Gülşan, M. E., R. Alzeebaree, A. A. Rasheed, A. Niş, and A. E. Kurtoğlu. Development of fly ash/slag based self-compacting geopolymer concrete using nano-silica and steel fiber. *Construction and Building Materials*, Vol. 211, 2019, pp. 271–283.
- [30] Althoey, F., O. Zaid, F. Alsharari, A. Yosri, and H. F. Isleem. Evaluating the impact of nano-silica on characteristics of self-compacting geopolymer concrete with waste tire steel fiber. Archives of Civil and Mechanical Engineering, Vol. 23, No. 1, 2023, pp. 1–17.
- [31] Xu, Z., H. Long, Q. Liu, H. Yu, X. Zhang, and D. Hui. Mechanical properties and durability of geopolymer concrete based on fly ash

- and coal gangue under different dosage and particle size of nano silica. *Construction and Building Materials*, Vol. 387, 2023, id. 131622.
- [32] Deb, P. S., P. K. Sarker, and S. Barbhuiya. Effects of nano-silica on the strength development of geopolymer cured at room temperature. Construction and Building Materials, Vol. 101, 2015, pp. 675–683.
- [33] Shehata, N., E. T. Sayed, and M. A. Abdelkareem. Recent progress in environmentally friendly geopolymers: A review. Science of The Total Environment. Vol. 762, 2021. id. 143166.
- [34] Amin, M., Y. Elsakhawy, and K. Abu, el-hassan, and B. A. Abdelsalam. Behavior evaluation of sustainable high strength geopolymer concrete based on fly ash, metakaolin, and slag. *Case Studies in Construction Materials*, Vol. 16, 2022, id. e00976.
- [35] A. C. C. O. Concrete and C. Aggregates, Standard specification for coal fly ash and raw or calcined natural pozzolan for use in concrete, ASTM International, West Conshohocken, PA, United States, 2013.
- [36] Assi, L. N., K. Carter, E. Deaver, and P. Ziehl. Review of availability of source materials for geopolymer/sustainable concrete. *Journal of Cleaner Production*, Vol. 263, 2020, id. 121477.
- [37] Tayeh, B. A., A. Hakamy, M. Amin, A. M. Zeyad, and I. S. Agwa. Effect of air agent on mechanical properties and microstructure of lightweight geopolymer concrete under high temperature. Case Studies in Construction Materials, Vol. 16, 2022, id. e00951.
- [38] Hassan, M. S. Adequacy of the ASTM C1240 specifications for nanosilica pozzolans. *The Open Civil Engineering Journal*, Vol. 13, No. 1, 2019, pp. 42–49.
- [39] Choudhary, R., R. Gupta, and R. Nagar. Impact on fresh, mechanical, and microstructural properties of high strength self-compacting concrete by marble cutting slurry waste, fly ash, and silica fume. *Construction and Building Materials*, Vol. 239, 2020, id. 117888.
- [40] Gupta, A. Investigation of the strength of ground granulated blast furnace slag based geopolymer composite with silica fume. *Materials Today: Proceedings*, Vol. 44, 2021, pp. 23–28.
- [41] Kansal, C. M. and R. Goyal. Effect of nano silica, silica fume and steel slag on concrete properties. *Materials Today: Proceedings*, Vol. 45, 2021, pp. 4535–4540.
- [42] P. Duan, C. Yan, W. Luo, and W. Zhou, Effects of adding nano-TiO₂ on compressive strength, drying shrinkage, carbonation and microstructure of fluidized bed fly ash based geopolymer paste. Construction and Building Materials, vol. 106, 2016, pp. 115–125.
- [43] Alomayri, T., A. Raza, and F. Shaikh. Effect of nano SiO2 on mechanical properties of micro-steel fibers reinforced geopolymer composites. *Ceramics International*, Vol. 47, No. 23, 2021, pp. 33444–33453.
- [44] Kim, M. J. and D. Y. Yoo. Cryogenic pullout behavior of steel fibers from ultra-high-performance concrete under impact loading. *Construction and Building Materials*, Vol. 239, 2020, id. 117852.
- [45] Li, T., Y. Zhang, and J. G. Dai. Flexural behavior and microstructure of hybrid basalt textile and steel fiber reinforced alkali-activated slag panels exposed to elevated temperatures. *Construction and Building Materials*, Vol. 152, 2017, pp. 651–660.
- [46] Kaplan, G., A. Öz, B. Bayrak, H. G. Alcan, O. Çelebi, and A. C. Aydın. Effect of quartz powder on mid-strength fly ash geopolymers at short curing time and low curing temperature. *Construction and Building Materials*, Vol. 329, 2022, id. 127153.
- [47] Rashad, A. M., A. A. Hassan, and S. R. Zeedan. An investigation on alkali-activated Egyptian metakaolin pastes blended with quartz powder subjected to elevated temperatures. *Applied Clay Science*, Vol. 132, 2016, pp. 366–376.
- [48] Aygörmez, Y. Evaluation of the red mud and quartz sand on reinforced metazeolite-based geopolymer composites. *Journal of Building Engineering*, Vol. 43, 2021, id. 102528.

- [49] A. C33/C33M-18. Standard specification for concrete aggregates, ASTM International, West Conshohocken, PA, USA, 2018.
- [50] Li, N., C. Shi, Z. Zhang, H. Wang, Y., and Liu. A review on mixture design methods for geopolymer concrete. Composites Part B: Engineering, Vol. 178, 2019, id. 107490.
- [51] Li, N., C. Shi, Z. Zhang, D. Zhu, H. J. Hwang, Y. Zhu, et al. A mixture proportioning method for the development of performance-based alkali-activated slag-based concrete. Cement and Concrete Composites, Vol. 93, 2018, pp. 163-174.
- [52] Aisheh, Y. I. A., D. S. Atrushi, M. H. Akeed, S. Qaidi, and B. A. Tayeh. Influence of polypropylene and steel fibers on the mechanical properties of ultra-high-performance fiber-reinforced geopolymer concrete. Case Studies in Construction Materials, Vol. 17, 2022, id. e01234.
- [53] Zeyad, A. M., K. H. Bayagoob, M. Amin, B. A. Tayeh, S. A. Mostafa, and I. S. Agwa. Effect of olive waste ash on the properties of highstrength geopolymer concrete. Structural Concrete, Vol. 25, No. 1, 2024, pp. 239-264.
- [54] Mousavinejad, S. H. G. and M. Sammak. Strength and chloride ion penetration resistance of ultra-high-performance fiber reinforced geopolymer concrete. Structures, Vol. 32, 2021, pp. 1420-1427.
- [55] Hattaf, R., M. Benchikhi, A. Azzouzi, R. El Ouatib, M. Gomina, A. Samdi, et al. Preparation of cement clinker from geopolymerbased wastes. Materials (Basel), Vol. 14, No. 21, 2021, id. 6534.
- [56] Ramasamy, S., K. Hussin, M. M. A. B. Abdullah, C. M. R. Ghazali, M. Binhussain, and A. V. Sandu. Interrelationship of kaolin, alkaline liquid ratio and strength of kaolin geopolymer. IOP Conference Series: Materials Science and Engineering, Vol. 133, 2016, id. 012004.
- [57] Wong, L. S. Durability performance of geopolymer concrete: A review. Polymers (Basel), Vol. 14, No. 5, 2022, id. 868.
- [58] Stacey, S. M. Evaluation of ASTM C 494 procedures for polycarboxylate admixtures used in precast concrete elements, ASTM International, West Conshohocken, PA, USA, 2016.
- [59] Naderi, M., A. Kaboudan, and A. Akhavan Sadighi. Comparative study on water permeability of concrete using cylindrical chamber method and British standard and its relation with compressive strength. Journal of Rehabilitation in Civil Engineering, Vol. 6, No. 1,
- [60] C. ASTM. Standard test method for electrical indication of concrete's ability to resist chloride ion penetration, ASTM International, West Conshohocken, PA, USA, C1202-18, 2012.
- [61] C. Astm. 1585–13 Standard test method for measurement of rate of absorption of water by hydraulic cement concrete, ASTM International, West Conshohocken, PA, 2013.
- [62] A. C/CM-18b. Standard test method for length change of hydrauliccement mortars exposed to a sulfate solution, ASTM International, West Conshohocken, PA, 2018.
- [63] Jindal, B. B. and R. Sharma. The effect of nanomaterials on properties of geopolymers derived from industrial by-products: A state-of-the-art review. Construction and Building Materials, Vol. 252, 2020, id. 119028.
- [64] Sastry, K. V. S. G. K., P. Sahitya, and A. Ravitheja. Influence of nano TiO2 on strength and durability properties of geopolymer concrete. Materials Today: Proceedings, Vol. 45, 2021, pp. 1017-1025.
- [65] Jagadesh, P. and V. Nagarajan. Effect of nano titanium di oxide on mechanical properties of fly ash and ground granulated blast furnace slag based geopolymer concrete. Journal of Building Engineering, Vol. 61, 2022, id. 105235.
- [66] Nuaklong, P., V. Sata, A. Wongsa, K. Srinavin, and P. Chindaprasirt. Recycled aggregate high calcium fly ash geopolymer concrete with inclusion of OPC and nano-SiO2. Construction and Building Materials, Vol. 174, 2018, pp. 244-252.

- [67] Jin, Q., P. Zhang, J. Wu, and D. Sha. Mechanical properties of nano-SiO2 reinforced geopolymer concrete under the coupling effect of a wet-thermal and chloride salt environment. Polymers, Vol. 14, No. 11, 2022, id. 2298.
- [68] Behfarnia, K. and M. Rostami. Effects of micro and nanoparticles of SiO2 on the permeability of alkali activated slag concrete. Construction and building materials, Vol. 131, 2017, pp. 205-213.
- [69] Huo, W., Z. Zhu, H. Sun, Q. Gao, J. Zhang, Y. Wan, et al. Reaction kinetics, mechanical properties, and microstructure of nano-modified recycled concrete fine powder/slag based geopolymers. Journal of Cleaner Production, Vol. 372, 2022, id. 133715.
- [70] Sanalkumar, K. U. A. and E. H. Yang. Self-cleaning performance of nano-TiO2 modified metakaolin-based geopolymers. Cement and Concrete Composites, Vol. 115, 2021, id. 103847.
- [71] Arunachelam, N., J. Maheswaran, M. Chellapandian, and T. J. S. Ozbakkaloglu. Effective utilization of copper slag for the production of geopolymer concrete with different NaOH molarity under ambient curing conditions. Sustainability, Vol. 14, No. 23, 2022, id. 16300.
- [72] Arunachelam, N., J. Maheswaran, M. Chellapandian, G. Murali, and N. I. J. S. Vatin. Development of high-strength geopolymer concrete incorporating high-volume copper slag and micro silica. Sustainability, Vol. 14, No. 13, 2022, id. 7601.
- Arunachelam, N., M. Chellapandian, J. Maheswaran, and G. Murali. [73] Strength and durability properties of alkali-activated concrete comprising glass fibers. In Advanced fiber-reinforced alkali-activated composites, Elsevier, Amsterdam, The Netherlands, 2023, pp. 359–380.
- [74] Abu el-Hassan, K., I. Y. Hakeem, M. Amin, B. A. Tayeh, A. M. Zeyad, I. S. Agwa, et al. Effects of nano titanium and nano silica on highstrength concrete properties incorporating heavyweight aggregate. Structural Concrete, Vol. 25, No. 1, 2023, pp. 239-264.
- Provis, J. L., R. J. Myers, C. E. White, V. Rose, and J. S. J. Van Deventer. X-ray microtomography shows pore structure and tortuosity in alkali-activated binders. Cement and Concrete Research, Vol. 42, No. 6, 2012, pp. 855-864.
- [76] Ibrahim, M., M. A. M. Johari, M. Maslehuddin, and M. K. Rahman. Influence of nano-SiO2 on the strength and microstructure of natural pozzolan based alkali activated concrete. Construction and Building Materials, Vol. 173, 2018, pp. 573-585.
- [77] Dheyaaldin, M. H., M. A. Mosaberpanah, and J. Shi. The effects of nanomaterials on the characteristics of aluminosilicate-based geopolymer composites: A critical review. Journal of Building Engineering, Vol. 73, 2023, id. 106713.
- [78] Deb, P. S., P. K. Sarker, and S. Barbhuiya. Sorptivity and acid resistance of ambient-cured geopolymer mortars containing nanosilica. Cement and Concrete Composites, Vol. 72, 2016, pp. 235-245.
- [79] Alani, A. H., N. M. Bunnori, A. T. Noaman, and T. A. Majid. Durability performance of a novel ultra-high-performance PET green concrete (UHPPGC). Construction and Building Materials, Vol. 209, 2019, pp. 395-405.
- [80] Amin, M., A. M. Zeyad, B. A. Tayeh, and I. S. Agwa. Effect of ferrosilicon and silica fume on mechanical, durability, and microstructure characteristics of ultra high-performance concrete. Construction and Building Materials, Vol. 320, 2022, id. 126233.
- [81] Atabey, İ. İ., O. Karahan, C. Bilim, and C. D. Atiş. The influence of activator type and quantity on the transport properties of class F fly ash geopolymer. Construction and Building Materials, Vol. 264, 2020, id. 120268.
- [82] Bakharev, T., J. G. Sanjayan, and Y. B. Cheng. Sulfate attack on alkali-activated slag concrete. Cement and Concrete Research, Vol. 32, No. 2, 2002, pp. 211-216.
- [83] Aisheh, Y. I. Palm oil fuel ash as a sustainable supplementary cementitious material for concrete: A state-of-the-art review. Case Studies in Construction Materials, Vol. 18, 2023, id. e01770.